applied sciences

MDPI

Article

A Master-Slave Separate Parallel Intelligent Mobile Robot Used for Autonomous Pallet Transportation

Guo Li [1], Rui Lin [2,*], Maohai Li [2], Rongchuan Sun [2] and Songhao Piao [1,*]

[1] Department of Computer Science and Technology, Harbin Institute of Technology, Harbin 150001, China; 14b903020@hit.edu.cn

[2] School of Mechanical and Electrical Engineering, Soochow University, Suzhou 215000, China; limaohai@suda.edu.cn (M.L.); sunrongchuan@suda.edu.cn (R.S.)

* Correspondence: linrui@suda.edu.cn (R.L.); piaosh@hit.edu.cn (S.P.)

Received: 27 December 2018; Accepted: 21 January 2019; Published: 22 January 2019

Abstract: This work reports a master-slave separate parallel intelligent mobile robot for the fully autonomous transportation of pallets in the smart factory logistics. This separate parallel intelligent mobile robot consists of two independent sub robots, one master robot and one slave robot. It is similar to two forks of the forklift, but the slave robot does not have any physical or mechanical connection with the master robot. A compact driving unit was designed and used to ensure access to the narrow free entry under the pallets. It was also possible for the mobile robot to perform a synchronous pallet lifting action. In order to ensure the consistency and synchronization of the motions of the two sub robots, high-gain observer was used to synchronize the moving speed, the lifting speed and the relative position. Compared with the traditional forklift AGV (Automated Guided Vehicle), the mobile robot has the advantages of more compact structure, higher expandability and safety. It can move flexibly and take zero-radius turn. Therefore, the intelligent mobile robot is quite suitable for the standardized logistics factory with small working space.

Keywords: intelligent mobile robot; pallet transportation; master-slave; compact driving unit; high-gain observer

1. Introduction

Logistics is an important part of the manufacturing enterprise [1,2], and the pallet is one of the logistics carriers in the factory [3]. The automation of pallet transportation is an important factor which affects the smart factory logistics [4]. Pallet handling equipment mainly refers to manually operated hydraulic trucks and electric or fuel forklifts, both of which require a large working space for operation. When the goods are delivered, it is necessary for the operator to handle the loading and unloading of the goods. A large amount of labor is required, which does not meet the requirements of factory automation.

In recent years, with the development of factory intelligence, flexible manufacturing systems and automated warehousing, the autonomous navigation forklift or forklift AGV (Automated Guided Vehicle) has gradually become an important device for solving the internal logistics of pallet transportation in the factory [5,6]. Compared with the traditional forklift, the autonomous navigation forklift AGV is improved with intelligent components such as external sensors, navigation and positioning modules, software scheduling, and power management system. Forklift AGV can transport the pallets placed on the ground to meet the unmanned logistics requirements [7–9]. As early as 2015, the forklift company, for example, Dematic or Jungheinrich, launched a forklift AGV based on the traditional forklift. For AGV products based on forklift, a single steering wheel or a differential fixed double steering wheel with a front integrated steering motor was generally used as the driving

wheel, and the two-forked casters with two auxiliary wheels. Forklift AGV could move freely by controlling a single steering wheel or a differential double steering wheel. Forklift AGV used the traditional forklift structure and had the function of stacking high pallets. However, due to its own structural characteristics, the overall size and its self-weight are both large. And the arrangement of the driving wheels and the attached wheels determined that this type of AGV cannot achieve zero-radius rotation. It requires a rather large working space [10].

In order to adapt to small working space of factory logistics, another type of pallet transportation robot was designed and used. The pallet transportation robot moved underneath the pallet rack to lift and delivered the pallet to a destination, which was placed on a pallet rack with a certain height in advance. In 2007, Professor Manuel Weber of the University of Stuttgart, Germany, proposed and designed the double-pronged pallet handling robot, the Doppelkufen system [11], to minimize the required transportation space. The Doppelkufen system used a visual recognition ribbon to guide between different production lines. In order to realize autonomous navigation, the two separate double forks connected with each other physically, and peripheral sensors were assembled to develop a compact forklift robot capable of zero-radius rotation and omnidirectional motion, for example, Agumos G130 [12] of Melkus Mechatronic GmbH and Nipper [13] of Dutch F3 Design. Combining with the advantages of both the traditional forklift AGV and the compact forklift AGV, INTREST Services GmbH of Germany introduced the Agilox product [14]. Agilox could perform palletizing automatically. It had a heavy self-weight and high height and cannot move underneath the pallet directly like a forklift. However the pallet needed to be placed on a custom-height pallet rack in advance.

In order to solve the problems, this paper mainly introduces a master-slave separate parallel intelligent mobile robot for autonomous pallet transportation in the smart factory logistics. The separate parallel intelligent mobile robot consists of two independent sub robots, which is similar to two forks of the forklift, but these sub robots do not have any physical connection with each other to achieve the pallet transportation. It can move underneath the narrow free entry of the pallet and has a load capacity of up to 1 ton. It was designed with a compact driving unit, in addition to actual motions, such as linear motion, oblique linear motion, and zero-radius turn. It could also perform synchronous lifting and laying of the pallet. The slave robot follows the master robot synchronously and consistently. Each robot had two driving units. In order to synchronize the motion and trajectory of these two sub robots, a nonlinear control system was used [15]. The application of nonlinear control systems in robotics control was very common, from the simplest two-wheel driving self-balancing robot dynamics [16,17], the robotic arm joint PD control [18], to the cluster control of UAV formations [19–21]. In the design we used the synchronic control strategy of slave robot dynamic adaptive following master robot. By analyzing the practical effects of sliding mode control [22] and high-gain observer [23] of the nonlinear control tools, we selected high-gain observer to obtain the following speed and state control of slave robot which was to ensure that the following errors converged and achieved synchronization of the master-slave robot motion.

Compared with the manual and forklift truck, the separate parallel intelligent mobile robot can fulfill an autonomous pallet transportation. Compared with the traditional intelligent forklift AGV, it has the advantages of compact structure, small self-weight and large payload, high expandability and safety. It can implement zero-radius turn and requires small channel width. It can also be combined with automation equipment or storage system seamlessly. So it is very suitable for small and standardized logistics warehouses.

The rest of this paper is organized as follows. Section 2 describes the mechanical structure of master-slave separate parallel intelligent mobile robot, such as compact driving units, communication modules, and safety protection modules. High-gain observer is adopted to ensure the consistency and synchronization of actual motions of two sub robots of intelligent mobile robot in Section 3. Experimental results and related analyses are given in Section 4, followed by conclusions in Section 5.

2. Separate Parallel Intelligent Mobile Robot

2.1. A Compact Driving Unit

As the EPAL Euro pallet is widely used in the factory logistics (PALETTE EUR-EPAL, dimension: L1200 mm × W800 mm and L1200 mm × W1000 mm), a compact driving unit was designed ensure that the two sub robots could move into the free entry of the standard pallet and lift the pallet up. Each sub robot has front and rear driving units. Separate parallel intelligent mobile robot implemented synchronous motions such as linear motion, oblique linear motion, and zero-radius turn. It could also perform synchronous lifting and laying of the pallet.

2.1.1. Motor Performance Calculation

In the actual motions of the master-slave separate parallel robot during the pallet transportation, it is necessary to overcome some resistance, such as the rolling resistance from the ground and the air resistance from the air. The resistance expressions $\sum F$ are:

$$\sum F = F_f + F_w + F_i + F_j \tag{1}$$

where, F_f is tolling resistance; F_w is air resistance; F_i is climbing resistance; F_j is acceleration resistance.

Tolling resistance for a sub robot is

$$F_f = \mu m g \tag{2}$$

where, μ is coefficient of tolling resistance. m represents the its own weight and maximum payload.

The resistance during acceleration of the sub robot is:

$$F_j = ma \tag{3}$$

Due to surface roughness, climbing resistance of the sub robot is

$$F_i = mg \sin \alpha \tag{4}$$

The rolling diameter of sub robot's driving wheel is set to D. The total motion-resistance force is $\sum F$. Then total resistance moment $\sum M$ is:

$$\sum M = \sum F \cdot \frac{D}{2} \tag{5}$$

As each unit has two driving wheels, the driving moment of every wheel M_d is

$$M_d = \frac{\sum M}{4} \tag{6}$$

According to the design requirements, a sub-robot's self-weight and maximum payload m = 600 kg. The normal velocity is 0.7 m/s. The acceleration is $a = 0.3$ m/s^2. The surface slope of working ground is $\alpha = 2^\circ$. The ground friction coefficient is $\mu = 0.02$.

2.1.2. Mechanism Design

Each sub robot uses front and rear driving units and one driving unit consists of two DC motors, reducers and driving wheels. The power transmission sequence is: DC motor, planetary reducer, small timing pulley, timing belt, large timing pulley, and driving wheel. The slip ring is assembled to simplify wiring during the zero-radius turn of the driving units. The slip ring is divided into upper and lower parts: the upper part is the stator, and the lower part is the rotor. The stator is fixed with the integral support plate, and the rotor rotates together with the driving mechanism. Slip ring not only solves the problem of wiring of power and cable during the lifting and laying of the pallet, but also

provides direction angle value for the front and rear driving units through the built-in multi-turn absolute encoder, which provides input for the nonlinear synchronization control in Section 3. It is known that the pitch, length and other parameters of the screw can lift the pallet up precisely to a certain height by controlling the number of wheel rotations of the driving units. Since the screw has a self-holding characteristic, the pallet does not fall down by itself even though power outage may occur unexpectedly. The compact driving unit is shown in Figure 1.

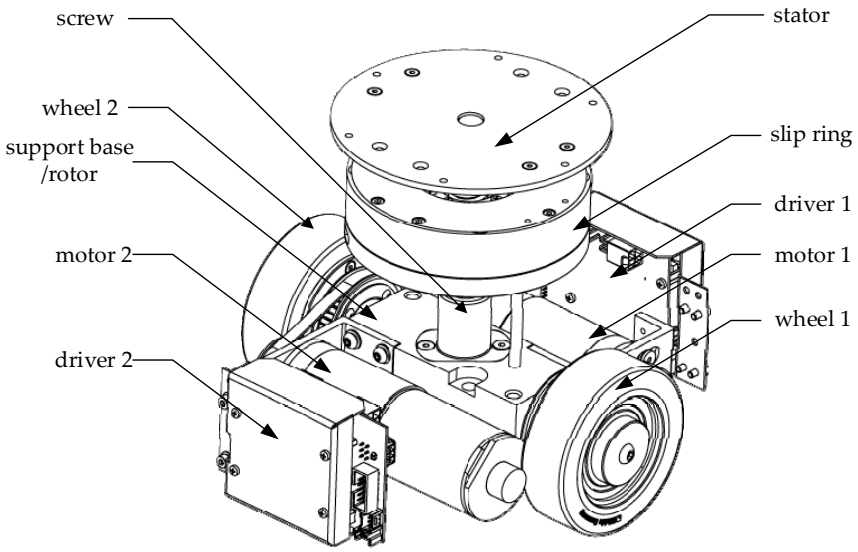

Figure 1. Three dimensional sketches of the compact driving unit.

2.1.3. Analysis of Motion Models

Motion models of separate parallel intelligent mobile robot are mainly based on the master robot's motion, such as visual navigation, and laser-based navigation. Slave robot follows master robot to dynamically adjust the relative speed and position. The two sub robots implement synchronous actual motions, such as linear motion, oblique linear motion, zero-radius turn, and lifting and laying. The motion model is shown in Figure 2.

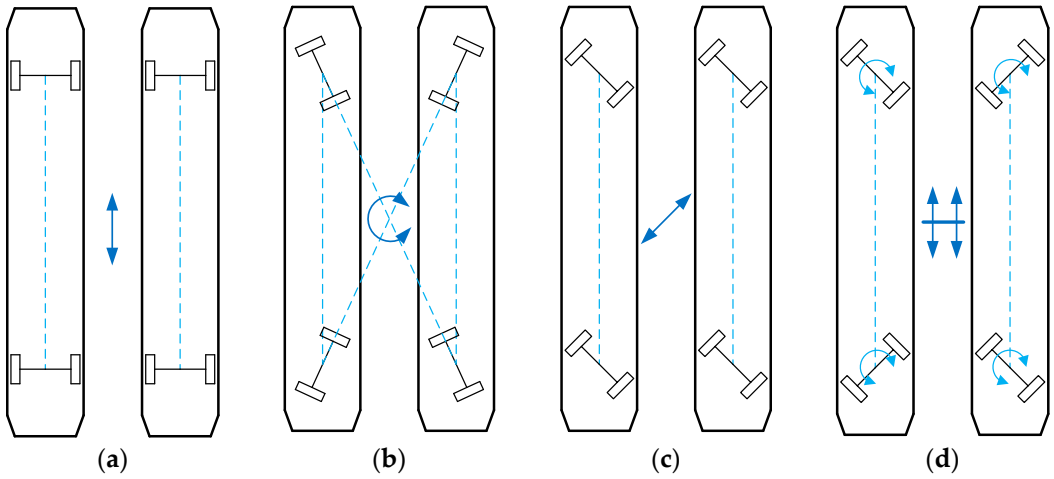

Figure 2. Analysis of motion model. (**a**) Forwards/Backwards; (**b**) Rotation; (**c**) Sideways/crab motion; (**d**) Lifting and laying.

2.2. Schematic Diagram of Separate Parallel Intelligent Mobile Robot

The main components of master-slave separate parallel intelligent mobile robot are: driving units, control and power supply modules, sensor modules, shell cover and safety protection modules, as shown in Figure 3. The individual modules of the sub robot are mechanically independent but electrically connected to each other. Each sub robot consists of two driving units, two safety protection modules, two sensor modules, and control and power supply modules with the cover. Safety sensors and infrared data transmission module are installed around the sides of each sub robot. The shell cover is the mounting base, and each module is mounted on the cover by a cross recessed countersunk head screw.

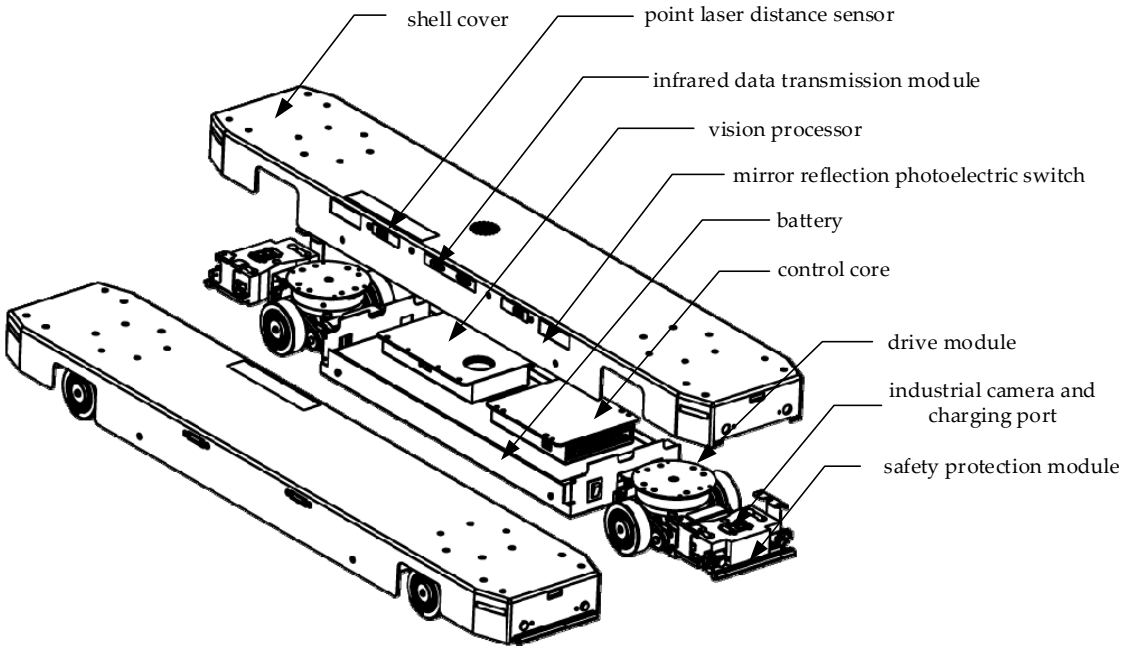

Figure 3. Schematic diagram of separate parallel intelligent mobile robot.

3. Synchronization Nonlinear Control

The most significant and complex problem in the real-time control system of the master-slave separate parallel intelligent mobile robot is the synchronization control of actual motions of the two sub robots, which is also a very difficult nonlinear control system. To get good performance of the synchronization control, complex nonlinear control strategy should be used. Therefore, this section mainly introduces some nonlinear control strategies, such as the input of nonlinear control system and high-gain observer control tool.

3.1. Control Strategies of Actual Motions

Different control strategies should be used in master robot and slave robot, while separate parallel intelligent mobile robot is moving. As the master robot, the only control principle is ensuring that the front and rear driving units work precisely and move as ordered. But for the slave robot, its control strategy is much more complex. (1) Self-motion conforms to self-physical model. (2) Following the master robot on front-rear axis and left-right axis, which are two different axes (X-axis and Y-axis). The repetitive position accuracy of master robot is normally distributed and related to the control accuracy of the driving units, the smoothness of the ground and the operation cycle time of the feedback control system. While the precision of driving wheel is higher and the smoothness of ground is better or the operation cycle time of control system is shorter, the variance of repetitive position accuracy will get smaller. As to the slave robot, the factors affecting repetitive position accuracy

are much more complex, which include master robot's position error, slave robot's following error, inherent errors, etc.

3.1.1. Control Strategy of Master Robot Motions

As mentioned above, master robot only needs to move according to the driving task demands. Therefore, PID control strategy is suitable for master robot to move to the destination or lift up and lay down the pallet by controlling its driving motors. What is more, in simulation diagram, module "Constant" means setting trajectory, and "Integrator" means that the odometer is the integral result of velocity and time. In "Control section", the speeds of the two driving units are adjusted dynamically based on the position feedback. Because the system is an open loop including integral part, a proportional part in feedback control can make master robot motion system gradually stable. Control strategy of master robot motion is shown in Figure 4.

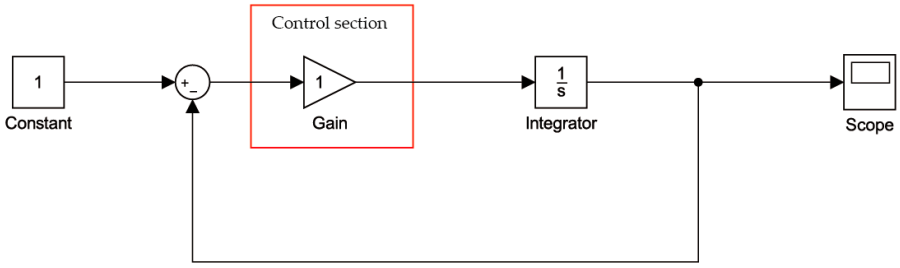

Figure 4. Control strategy of master robot motion.

3.1.2. Control Strategy of Slave Robot Motions

In fact, slave robot control system is a very complex nonlinear control strategy. Here, the main control ideas of slave robot are described in this section. The controlled object for slave robot are driving units. Control goal is to eliminate position errors on X-axis and Y-axis. The feedback signal includes the distance data between master robot and slave robot, and the SIGN signal indicates if master robot position leads or lags on Y-axis.

In order to keep the system in a steady stable state, the system's energy derivative should be non-positive definite according to Lyapunov's second stability theorem. Therefore, in this control system the driving motors' speed should tend to be stable in the process of system. Because slave robot cannot know the accurate error in real time between master robot and slave robot on Y-axis, which means it is impossible for slave robot to follow master robot without position error on Y-axis. Therefore, high-gain observer is used for keep slave robot stable within a certain error value while following master robot on Y-axis. Actually, when high-gain observer is used, it will affect the motions on both X-axis and Y-axis. Because when driving units move in the oblique linear direction, slave robot motion on X-axis and Y-axis are coupling. The slave robot moving on Y-axis will also result in moving on X-axis. Therefore, high-gain observer should be used when slave robot motion on X-axis and-Y axis are in the positive correlation.

In order to assure the sub robot motion on X-axis and Y-axis are in positive correlation, the moving direction of driving units should be adjusted accordingly. Because the control system energy will not be changed if only directions of driving units are adjusted. In fact, by adjusting driving motors' direction, the motions on X-axis and Y-axis are able to be changed as ordered. By using the above control strategy, the following errors between master robot and slave robot will be converged, and slave robot is able to keep stable within a certain error range. The control strategy of slave robot is shown in Figure 5.

Given the initial position offset and angle offset, the errors on X-axis and Y-axis will approach zero but not reaches an asymptotically stability using high-gain observer control strategy. In the actual motions, the following errors between master robot and slave robot can be observed by industrial

camera. And jitters may occur during slave robot motion, which also verifies the accuracy of high-gain observer control tool.

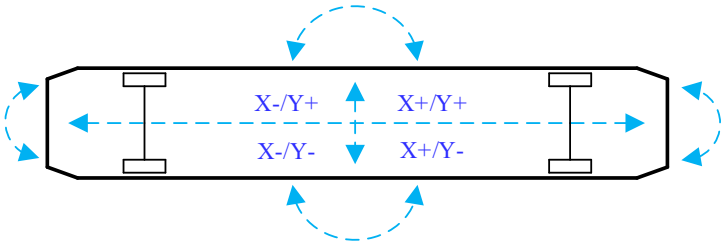

Figure 5. Control strategy of slave robot.

3.2. Input of Nonlinear Control System

Separate parallel intelligent mobile robot uses master-slave robot structure. In order to achieve high performance of real-time control and response, the chip with over 600 MHZ main frequency should be selected as main control chip. What is more, RTOS system should be embedded for using time slices efficiently. And infrared data transmission module is used for real-time communication between master robot and slave robot. In this way, the operation cycle time of the control system can be within 5 milliseconds, which is an important factor of affecting master-slave robot real-time synchronization control.

In order to reduce the following errors and achieve high repetitive position accuracy, high-precision sensors should be used, for example distance sensors. In this way, sensors will get relative distance data, which are also the input parameters of slave robot nonlinear control system. Here are the input parameters of slave robot nonlinear control system:

(1) Distance between master robot and slave robot on X-axis: the precise distance between slave robot and master robot can be obtained by two sets of high-precision point laser distance sensors which are installed on the relative side of the front and rear of slave robot.

(2) Distance between master robot and slave robot on Y-axis: position error on Y-axis can be roughly measured by tree groups of mirror reflection photoelectric switches, which return a set of SIGN function signal to the control system. That is to say, if the difference between slave robot and master robot is greater than a preset value, the Y-axis distance sensor returns +1 signal to the control system. If the difference is within a preset range, the Y-axis distance sensor returns 0 signal to the control system. Otherwise, the Y-axis distance sensor returns -1 signal.

Obviously, the procedure of slave robot following master robot is a nonlinear control process. The input parameters of the nonlinear control system include the distance on X-axis and position error SIGN signal on Y-axis. And the output is the moving speed of each driving motor. The goal of the slave robot control system is to make the following process stable and keep the following errors between master robot on X-axis and Y-axis within a preset value.

3.3. High-Gain Observer

High-gain observer is a good tool for the nonlinear control process in which some state variables cannot be measured accurately due to technical or economic reasons. In some practical cases, the tool can be modified to produce an output feedback controller [14].

Suppose that a nonlinear system can be transformed into the form:

$$\begin{cases} \dot{x} = Ax + g(y, u) \\ \hat{y} = Cx \end{cases} \tag{7}$$

where (A, C) is observable. This form is special because the nonlinear function g depends only on the output y and the control input u. Taking the observer as:

$$\dot{\hat{x}} = A\hat{x} + g(y, u) + H(y - C\hat{x}) \tag{8}$$

it can be easily seen that the estimation error $\tilde{x} = x - \hat{x}$ satisfies the linear equation:

$$\dot{\tilde{x}} = (A - HC)\tilde{x} \tag{9}$$

Hence, designing H such that $A - HC$ is Hurwitz guarantees asymptotic error convergence, that is $\lim_{x\to\infty} \tilde{x}(t) = 0$. Aside from the fact that the observer works only for a special class of nonlinear systems, its main drawback is the assumption that the nonlinear function g is perfectly known. Any error in modeling g will be reflected in the estimation error equation.

The upper nonlinear observer is suitable for most system. But for the sub-style parallel intelligent mobile robot, slave robot should follow master robot synchronously and timely. There are also many measurement deviations. We should give a special design of the observer gain that makes the observer robust to uncertainties in modeling the nonlinear functions. High-gain observer can guarantee that the output feedback controller recovers the performance of the state feedback controller when the observer gain is sufficiently high.

We use the observer in output feedback stabilization. The main results in Section 4 are separation principles that allow us to separate the design into two tasks. First, we design a state feedback controller that stabilizes the system and meets other specifications. Then, an output feedback controller is obtained by replacing the state x by its estimate $\hat{x}$ provided by high-gain observer. A key property that makes this separation possible is the design of the state feedback controller to be globally bounded in x. High-gain observer can be used in a wide range of control problems.

Consider the second-order nonlinear system:

$$\begin{cases} \dot{x}_1 = x_2 \\ \dot{x}_2 = \phi(x, u) \\ y = x_1 \end{cases} \tag{10}$$

where $x = [x_1, x_2]^T$. Suppose $u = y(x)$ is a locally Lipschitz state feedback control law that stabilizes the origin $x = 0$ of the closed-loop system.

To implement this feedback control using only measurements of the output y, we use the observer:

$$\begin{cases} \dot{\hat{x}}_1 = \hat{x}_2 + h_1(y - \hat{x}_1) \\ \dot{\hat{x}}_2 = \phi_0(\hat{x}, u) + h_2(y - \hat{x}_1) \end{cases} \tag{11}$$

We set $\tilde{x}_1(0) = 0$ and $\tilde{x}_2(0) = 0$. Where $\phi_0(x, u)$ is a nominal model of the nonlinear function $\phi(x, u)$. The estimation error:

$$\tilde{x} = \begin{bmatrix} \tilde{x}_1 \\ \tilde{x}_2 \end{bmatrix} = \begin{bmatrix} x_1 - \hat{x}_1 \\ x_2 - \hat{x}_2 \end{bmatrix} \tag{12}$$

Satisfies the equation:

$$\begin{cases} \dot{\tilde{x}}_1 = -h_1\tilde{x}_1 + \tilde{x}_2 \\ \dot{\tilde{x}}_2 = -h_2\tilde{x}_1 + \delta(x, \tilde{x}) \end{cases} \tag{13}$$

where $\delta(x, \widetilde{x} = \phi(x, \gamma(\hat{x})) - \phi_0(\hat{x}, \gamma(\hat{x})))$. We want to design the observer gain $H = [h_1, h_2]^T$ such that $\lim_{t\to\infty}\widetilde{x}(t) = 0$. In the absence of the disturbance term δ, asymptotic error convergence is achieved by designing H such that:

$$A_o = \begin{bmatrix} -h_1 & 1 \\ -h_2 & 0 \end{bmatrix} \tag{14}$$

is Hurwitz. For this second-order system. A_o is Hurwitz for any positive constants h_1 and h_2. In the presence of δ, we need to design H with the additional goal of rejecting the effect of δ on x. This is ideally achieved, for any δ, if the transfer function:

$$G_o(s) = \frac{1}{s^2 + h_1 s + h_2}\begin{bmatrix} 1 \\ s + h_1 \end{bmatrix} \tag{15}$$

From δ to x is identically zero. While this is not possible, we can make $\sup_{\omega\in R}|G_o(j\omega)$ arbitrarily small by choosing $h_2 >> h_1 >> 1$. In particular, taking

$$h_1 = \frac{\alpha_1}{\varepsilon}, h_2 = \frac{\alpha_2}{\varepsilon^2} \tag{16}$$

for some positive constant α_1, α_2 and ε, with $\varepsilon << 1$, it can be shown that:

$$G_o(s) = \frac{\varepsilon}{(\varepsilon s)^2 + \alpha_1 \varepsilon s + \alpha_2}\begin{bmatrix} \varepsilon \\ \varepsilon s + \alpha_1 \end{bmatrix} \tag{17}$$

Hence, $\lim_{\varepsilon\to 0} G_o(s) = 0$. The disturbance rejection property of high-gain observer can be also seen in the time domain by representing the error equation in the singularly perturbed form.

The initial conditions are $\varepsilon = 0.01$, $h_1 = 100$, and $h_2 = 1000$. We can obtain the best high-gain observer for synchronization control of these two sub robots of separate parallel intelligent mobile robot.

4. Experiment and Analysis

The separate parallel intelligent mobile robot consists of two independent sub robots, a master robot and a slave robot, which are similar to two forks of the forklift, but the sub robot does not have any physical connection with master robot. Each robot has front and rear driving units. These two sub robots collaborate to deliver the pallet synchronously. This section will analyze the steady state error in order to synchronize the actual motions of these two sub robots. The center of gravity distribution and offset error during flexible docking to the free entry of the pallet will be also analyzed.

4.1. Steady State Error Analysis of Actual Motions

This section will summarize the steady state error of actual motions based on both simulation in Simulink and convergence of results.

4.1.1. Linear Motion

When the master-slave mobile robot is moving linearly frontwards or backwards, slave robot should follow master robot synchronously. In order to get the value of front or rear deviation, three non-uniformly distributed are used to get relative position, which is set to be SIGN (+1, −1, 0). Slave robot should align its velocity of every driving motor by high-gain observer in real time. Otherwise, jitter of slave robot will be intolerable. Then slave robot cannot follow master robot synchronously. The procedure of adjusting relative velocity and position will be convergent and easy to reach a steady state after a period of time. The jitter of slave robot following master robot will also be reduced. The simulation in Simulink and convergence of results are shown in Figure 6. As shown in Figure 6b,

there are following errors at the beginning of linear motion. In Figure 6b, the abscissa unit is second and ordinate unit is millimeter. Self-adjusting process during the following procedure will then eliminate.

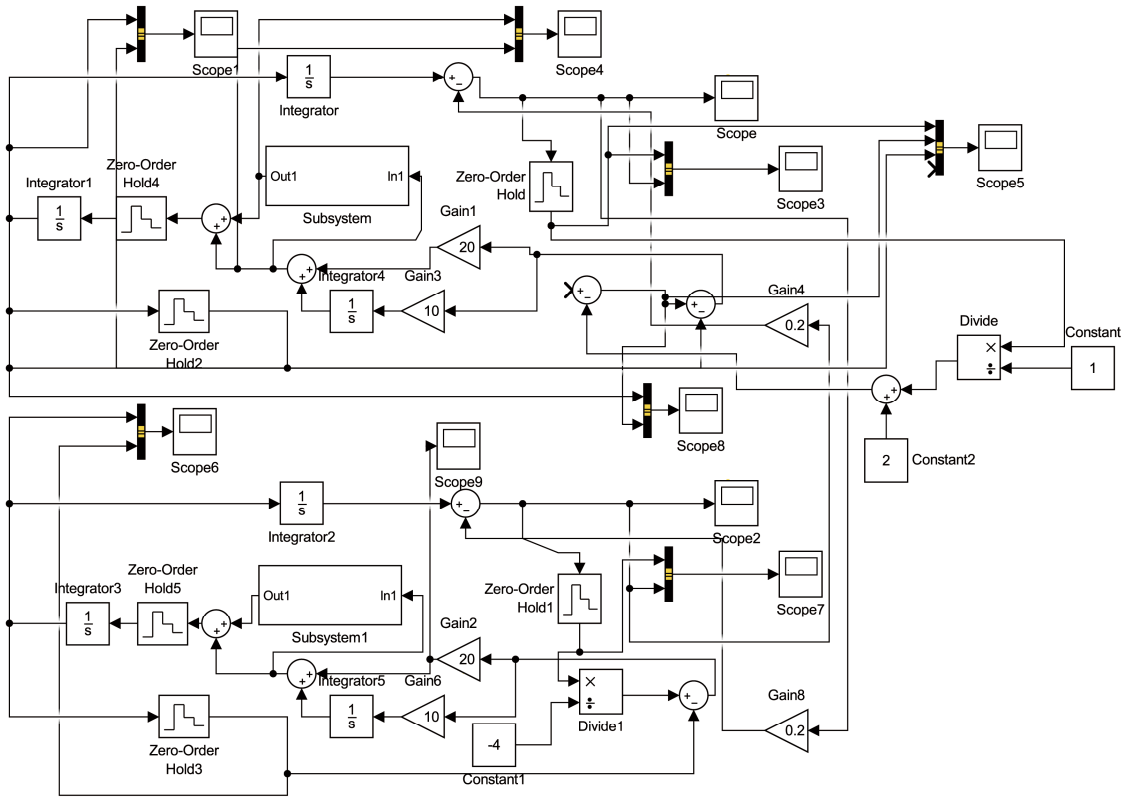

(**a**)

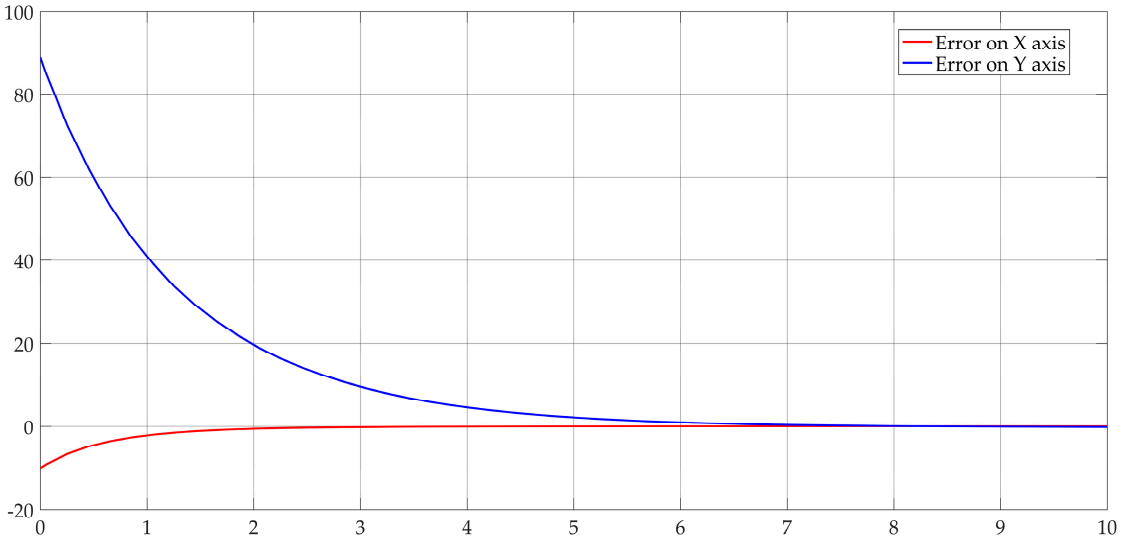

(**b**)

Figure 6. The simulation in Simulink and convergence of results for linear motion. (**a**) Simulink simulative model graph; (**b**) The model reaches a steady convergent state.

4.1.2. Oblique Linear Motion

Integrator and *integrator1* are two integrations of the model which describe the driving motor of the sub robot. Also this represents that the speed difference of driving motors would not directly

cause the offset of robot motion. Simple Zero-Order-Hold is sample hold. Due to the integral element could lead to time-delay and vibration, the system would not use integral element in system offset reducing. So only *integrator4* is added to I in outer-loop in Simulink to reduce steady state error in the actual following motions. Theoretically, when the initial offset of following motion is 15 mm and angle is $-5°$, the following errors on X-axis and Y-axis will approximate 0 after reaching the steady state. As shown in Figure 7, the model reaches a steady convergent state. In Figure 7b, the abscissa unit is second and ordinate unit is millimeter.

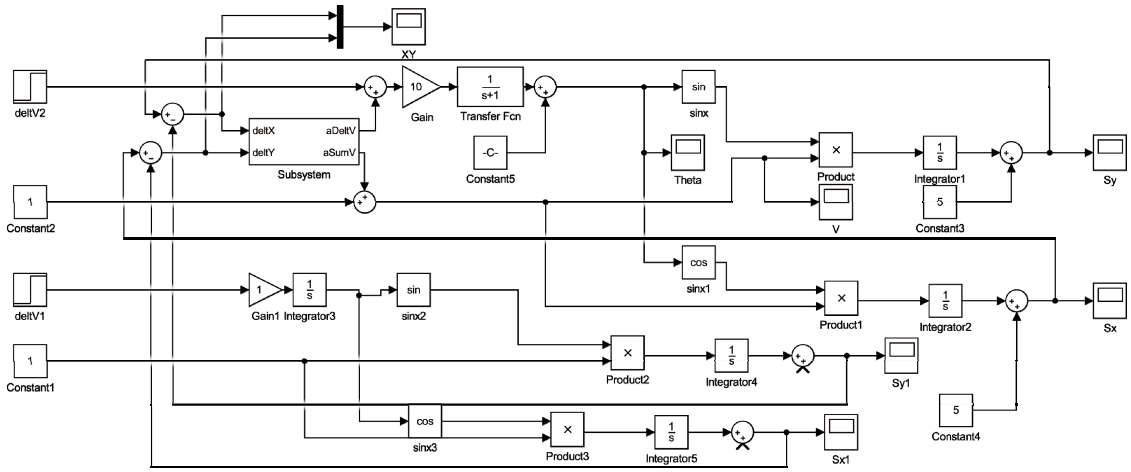

(**a**)

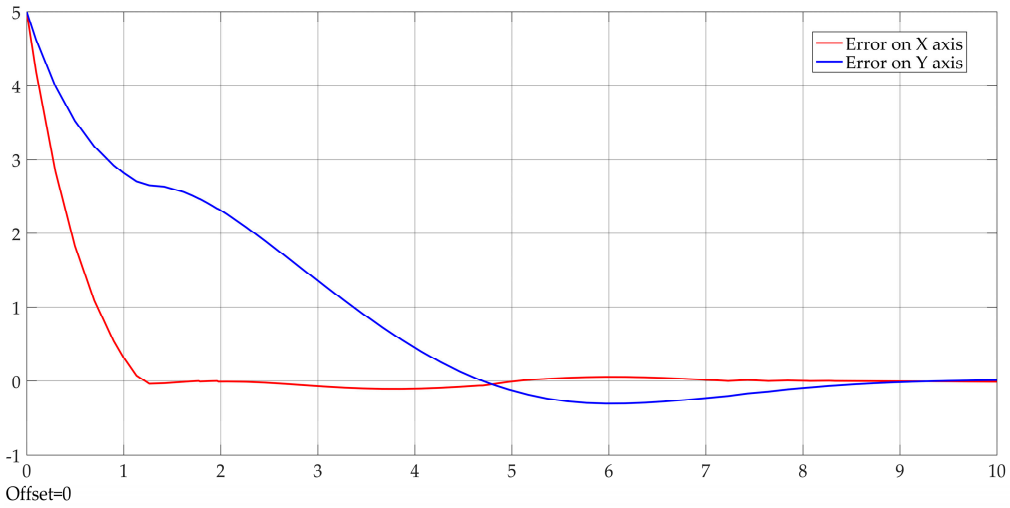

(**b**)

Figure 7. The simulation in Simulink and convergence of results for oblique linear motion. (**a**) Simulink simulative model graph; (**b**) The model reaches a steady convergent state.

4.1.3. Zero-radius Turn

When the master-slave separate parallel intelligent mobile robot takes a zero-radius turn, slave robot should follow master robot's position synchronously and timely on both X-axis and Y-axis. While rotating, the motion analysis of driving units should have a unique solution in the robot motion model. Then the velocities of slave robot's front and rear driving motors will cancel out each other on Y-axis. And the velocity on X-axis of the sub robot's driving motors is taken as the linear velocity while rotating. When the position following errors on X-axis and Y-axis occur on slave robot, the velocity and direction of driving units should be adjusted in real time, by using Lyapunov second stability theorem. It should be noted that when slave robot is adjusted, it is not guaranteed that both the position

following errors on X-axis and Y-axis converge simultaneously. However the energy derivative of control system is always non-position define. The simulation in Simulink and convergence of results for zero-radius turn are shown in Figure 8. In Figure 8b, the abscissa unit is second and ordinate unit is millimeter.

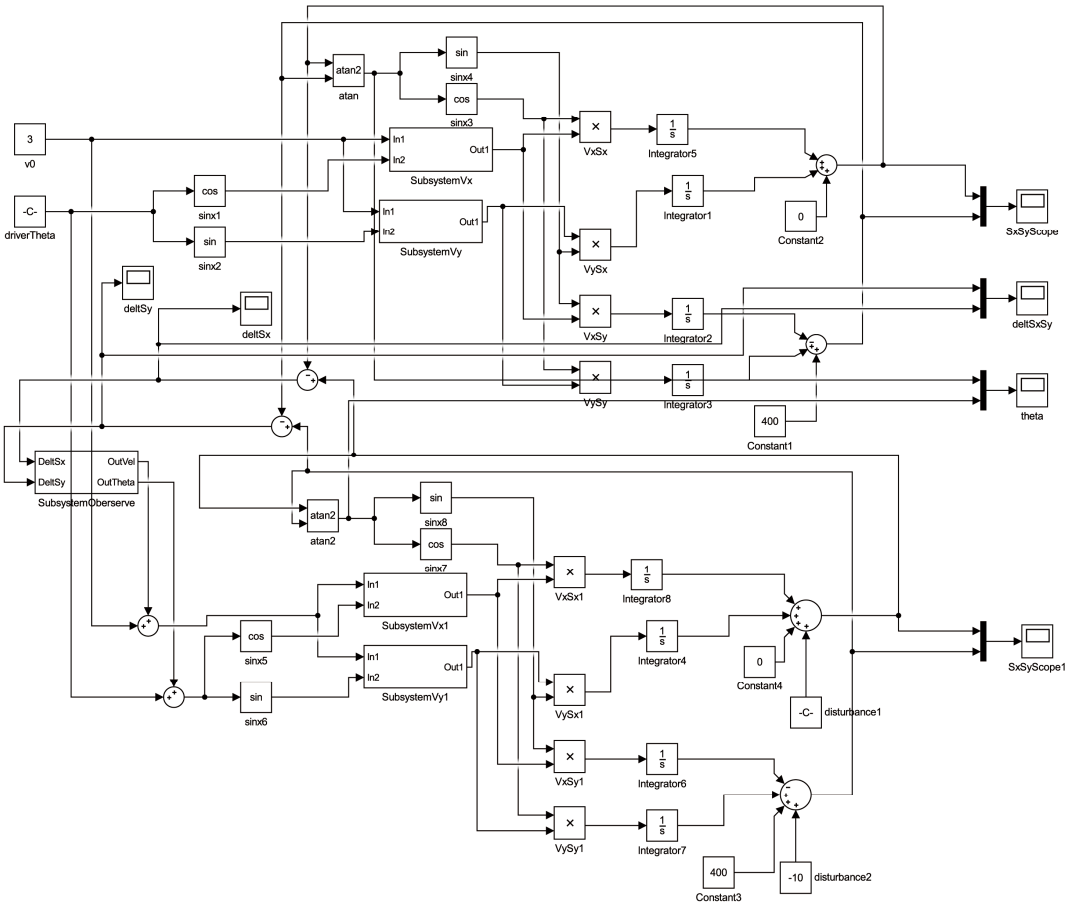

(**a**)

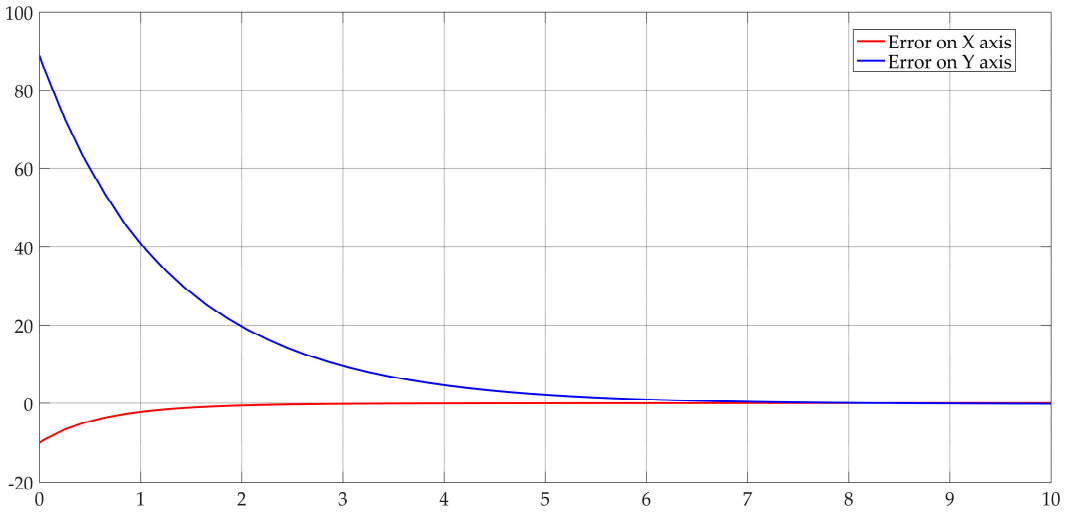

(**b**)

Figure 8. The simulation in Simulink and convergence of results for zero-radius turn. (**a**) Simulink simulative model graph; (**b**) The model reaches a steady convergent state.

4.1.4. Steady State Error Factors

As we know, in the ideal case, the zero offset error means that slave robot follows master robot absolutely according to calibrated data, and there is no error. So the most significant factor that affects the stability of the system is the accuracy of calibrated data. (1) Camera installation error: The installation angle deviation of camera and driving unit is unavoidable. The camera should be calibrated first to reduce the initial angle deviation. (2) Encoder calibration offset: The error of encoder deviation would be transferred from inner-loop to the outer-loop. Thus the encoder calibration offset would directly lead to the error of system stability. (3) Accuracy of driving control: In actual motions, the precision of each driving motor is up to 1 rpm. As the result, the precision of the following velocity and position control could not be well guaranteed. (4) Mechanical installation error: The mechanical installation error represents installation tolerance error such as driving unit and other mechanical parts. All these errors would result in the difference between calibrated zero position and actual zero position.

As we known, the errors of actual motions of these two sub robots cannot reach zero. This section analyzes most of the factors that may affect the steady state errors of the following motions. The two driving units of slave robot may jitter during the adjusting control. Surface roughness of the road and the curve degree of vision-based color bar on the road can both have significant effect on the stability of the master-slave parallel robot' motion. As discussed above, various factors affect the steady state error. The steady state error for the master-slave mobile robot measured in the experiment is about 3mm, which is not easy to eliminate.

4.2. Accurate Flexible Docking to the Free Entry of the Pallet

To ensure that the two sub robots can move underneath the pallet accurately and lift up and lay down the pallet synchronously, an evaluation of docking to the free entry is required. After arriving at the pre-docking position, the mobile robot should recognize and compute the accurate position the free entry of pallet by laser sensor or vision sensor, and then move into the free entry smoothly. In this section, the maximum deviation angle error $\beta_{\max}$ during docking to the free entry is analyzed through synthetical consideration of the following error and positioning error.

4.2.1. The Ideal Case (No Direct Collision)

In order to lift the pallet up, the sub robot should move underneath the pallets accurately and safely. In the ideal case, the shell cover of the sub robot won't collide with the edge of the free entry of the pallets, as shown in Figure 9a. $\beta_1 = (90^\circ - \theta_1)$ represents the intersection angle of the sub robot and the free entry of the pallet.

$$\begin{cases} AC = l_r - \frac{w_r - w_h}{2} \tan\delta \\ BC = \frac{w_p - w_r}{2} \pm \varepsilon \\ \cos\theta_1 = \frac{BC}{AC} \end{cases} \tag{18}$$

where, $l_r = 1180$ mm is the length of the basis of the sub robot. $w_r = 212$ mm is the width of the basis of the sub robot. $w_h = 170$ mm is the width of the head of the sub robot. $\delta = 70^\circ$ is the conical chamfer of the head of the sub robot. $w_p = 382.5$ mm represents the width of free entry of the pallet. $\varepsilon = 10$ mm is the maximum following error of the sub robot.

Relative deviation angle β_1:

$$3.84^\circ < \beta_1 = (90^\circ - \theta_1) < 4.87^\circ \tag{19}$$

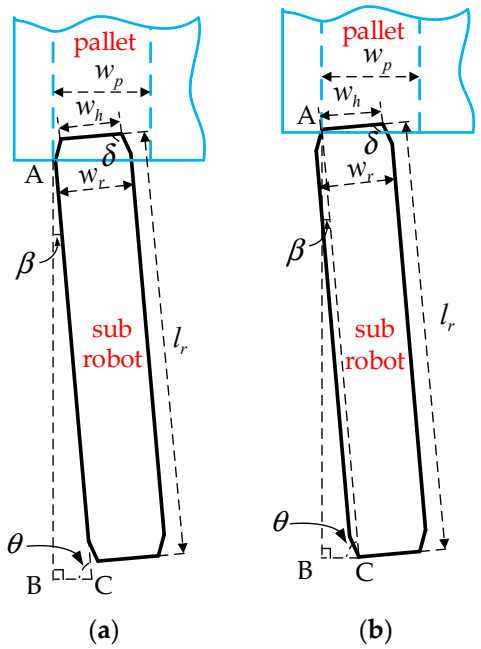

Figure 9. The maximum deviation angle error of a sub robot docking to the free entry of the pallet. (**a**) The ideal case; (**b**) The extreme case.

4.2.2. The Extreme Case (Contact Guidance)

Although the shell cover of the sub robot will collide with the free entry slightly in some conditions, the sub robot can move underneath the pallets yieldingly, as shown in Figure 9b. $\beta_2 = (90^\circ - \theta_2)$ represents the included angle of the sub robot and the free entry of the pallet.

$$\begin{cases} AC = l_r \\ BC \approx \frac{l_r - w_r}{2} + \frac{w_r - w_h}{2} \pm \varepsilon \\ \cos\theta_2 = \frac{BC}{AC} \end{cases} \tag{20}$$

Relative deviation angle β_2:

$$4.70^\circ < \beta_2 = (90^\circ - \theta_2) < 5.65^\circ \tag{21}$$

By combing Equation (19) with (21), we have the the maximum allowable angle error $\beta_{\max}$:

$$-\max(\beta_1, \beta_2) < \beta_{\max} < \max(\beta_1, \beta_2) \tag{22}$$

Therefore, $\beta_{\max} \in \begin{pmatrix} -5.65^\circ & 5.65^\circ \end{pmatrix}$.

4.3. Analysis of Lifting and Laying

The main procedures of pallet transportation for intelligent mobile robot are that it firstly moves underneath the pallet, then lifts the pallet up and delivers the pallet to the destination, and finally lays it down. In order to control motions of the two sub robots synchronously, this section analyzes the pallet offset error, including longitudinal and transverse offset error during lifting and laying.

4.3.1. Analysis of Center of Gravity

As we know, the sub robot may roll over while the four driving motors are at two parallel lines at a certain moment. Relative velocity and position control loops are used during the lifting and laying of the pallet. The front and rear driving wheels are always vertical through position feedback. The initial

relative angle of front and rear driving units is shown in Figure 10. Thus the center of gravity of robot will be within the base of the sub robot during the procedure of lifting and laying.

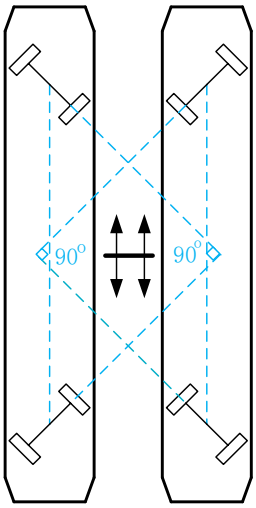

Figure 10. The initial relative angle of front and rear driving units before lifting and laying.

4.3.2. Analysis of Pallet Offset Error

During the lifting process, the offset errors of the position of the pallet include longitudinal offset error and transverse offset error. They are both caused by uneven ground and jittering of sub-robot's motion. It is difficult to guarantee the level of the ground, so changing or optimizing the robot motion is the most effective way.

- Analysis of pallet longitudinal offset errors

The longitudinal offset errors of the pallet cannot be completely eliminated. It is unable to measure the absolute accurate deviation between pallet position and robot position, so no correction can be made. There must be cumulative error between them. What we should do is to ensure the absolute stop position between lifting and laying as consistent as possible. The two sub robots should be controlled to stop accurately and synchronously while height position of the pallet changes. The control strategy of accurate stop is shown in Figure 11.

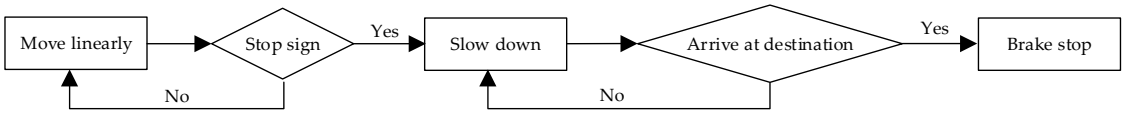

Figure 11. Control strategy of accurate stop.

- Analysis of pallet transverse offset errors

The transverse offset of the pallet refer to errors in the left and right direction. In general, the mobile robot moves underneath of the pallet and then lift the pallet up. But once there are some transverse offset errors, the mobile robot may be stuck under the free entry of the pallet. It may be caused by uneven ground or jitters of the sub robot's motions. In order to reduce the transverse offset errors, dynamic position adjustment is required during lifting and laying. The dynamic adjustment strategy is shown in Figure 12. The rotation angle of each driving unit is divided into 2 areas. (1) Angle adjustment areas. If the angle of rear driving unit is in the range of angle that needs to be adjusted, the rear driving unit will follow the front one, and they will be perpendicular. Within the angle adjustment areas, the center of gravity of the sub robot can always maintain a relatively large area, which will prevent the sub robot to roll over. (2) Position adjustment areas. If the angle of driving unit is in the

range of position that needs to be adjusted, the speed of the driving motor will be changed according to the position error collected by the camera or navigation sensor. It ensures that the sub robot performs left and right position feedback during the procedure of lifting and laying. According to the position adjustment areas, it is possible to optimize the transverse offset errors between the sub robot and the pallet.

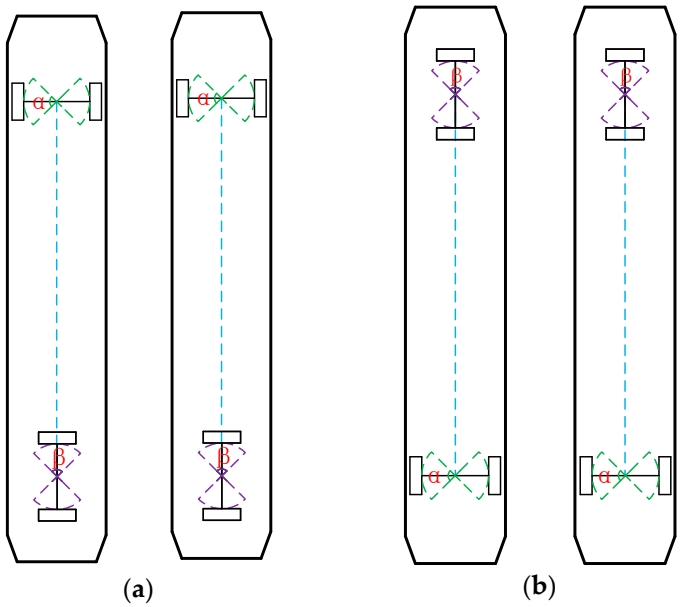

Figure 12. Dynamic adjustment strategy of master-slave robot during lifting and laying. (**a**) Angle adjustment areas; (**b**) Position adjustment areas.

When the front or rear driving unit lies in the angle adjustment area, we adjust the speeds of the two motors of this driving unit synchronously. The two motors may accelerate or decelerate at the same speeds. But when the front or rear driving unit lies in the position adjustment area, we adjust the speeds of the two motors of this driving unit asynchronously. The two motors may accelerate or decelerate at the different speeds.

4.4. Actual Running Performance

The master-slave separate parallel intelligent mobile robot was designed and assembled. The performance was tested by actual delivering the pallets in the factory. The two sub robots could also lift up and lay down the pallet synchronously. The mobile robot moved flexibly at the crossroads. And detailed specifications of the master-slave separate parallel intelligent mobile robot are listed in Table 1.

Table 1. The specifications of the master-slave separate parallel intelligent mobile robot.

Feature	Specification	Feature	Specification
max payload	1000 kg	swing radius	>730 mm
max speed	0.7 m/s	navigation	color bar/vision
outline dimension	L1180 × W212 × H98 mm	running time	10 h
weight	40 kg	charging time	2 h
uplift height	28 mm	turning radius	0 mm
uplift time	16 s	pallets	PALETTE EUR-EPAL

5. Conclusions

To pick up and transport pallets autonomously in the factory, a master-slave separate parallel intelligent mobile robot was designed. The mobile robot consists of two independent sub robots, which

are similar to two forks of the forklift, but master robot does not have any physical connection with slave robot. In order to adapt to the compact space of the entry of pallet, four compact motion driving units are designed for these two sub robots. High-gain observer is used to control the following speed timely. The state control of slave robot is to ensure that the following error converges and achieve synchronization of the two sub robots' motions. The experiment results demonstrate that the separate parallel intelligent mobile robot can transport the pallet autonomously. The two sub robots can fulfill synchronous motions, such as linear motion, oblique linear motion, and zero-radius turn. They can also lift up and lay down the pallet synchronously. The mobile robot moves flexibly and is quite suitable for the standardized logistics factory with small working space. In our future research, the autonomous navigation module based on the 2D laser will be assembled with the intelligent mobile robot. Then the mobile robot can move freely for pallet transportation in the factory.

Author Contributions: Data curation, G.L. and R.L.; Formal analysis, R.S.; Investigation, M.L. and R.S.; Methodology, R.L., M.L. and S.P.; Project administration, S.P.; Software, G.L.; Writing—original draft, R.L.; Writing—review & editing, R.L. and S.P.

Funding: This research was funded by the Projects of the National Natural Science Foundation (61673288).

Acknowledgments: Thanks associate Professor Hongmiao Zhang for giving suggestions to improve this manuscript. We would like to take the opportunity to thank the reviewers for their thoughtful and meaningful comments.

Conflicts of Interest: The authors declare no conflict of interest.

References

1. Behzad, E.; Sara, B.; Ben, W. The evolution and future of manufacturing: A review. *J. Manuf. Syst.* **2016**, *39*, 79–100.
2. Jeremie, C. *A Look into Logistics Automation. ROBO Global Defining the Universe of Robotics and Automation*; ETF Securities: London, UK, 2017; pp. 1–18.
3. Paweł, Z. Model of Forklift Truck Work Efficiency in Logistic Warehouse System. In *Logistics Operations, Supply Chain Management and Sustainability*; Springer: Cham, Switzerland, 2014; pp. 467–479.
4. Armesto, L.; Tornero, J.; Torres, J. Transport process automation with industrial forklifts. *IFAC Proc.* **2003**, *36*, 33453–33455. [CrossRef]
5. Kelen, C.T.; Marcelo, B.; Glauco, A.P. Automatic routing of forklift robots in warehouse applications. *ABCM Symp. S. Mechatron.* **2010**, *4*, 335–344.
6. Wang, J.; Zhang, N.; He, Q. Application of Automated Warehouse Logistics in Manufacturing Industry. In Proceedings of the IEEE 2009 ISECS International Colloquium on Computing, Communication, Control, and Management, Sanya, China, 8–9 August 2009.
7. Li, L.Y.; Liu, Y.H.; Fang, M.; Zheng, Z.-Z.; Tang, H.-B. Vision-Based Intelligent Forklift Automatic Guided Vehicle (AGV). In Proceedings of the 2015 IEEE International Conference on Automation Science and Engineering (CASE), Fort Worth, TX, USA, 21–24 August 2015; pp. 264–265.
8. Seelinger, M.; Yoder, J.D. Automatic Pallet Engagment by a Vision Guided Forklift. In Proceedings of the 2005 IEEE International Conference on Robotics and Automation, Barcelona, Spain, 18–22 April 2005.
9. Qian, J.; Zi, B.; Wang, D.; Ma, Y.; Zhang, D. The Design and Development of an Omni-Directional Mobile Robot Oriented to an Intelligent Manufacturing System. *Sensors* **2017**, *17*, 2073. [CrossRef] [PubMed]
10. Patel, P.; Parekh, R.; Panchal, R.; Solanki, V. Material Handling System Based on Automated Guided Vehicle: Scope, Limitation and Application. In Proceedings of the International Conference on Emerging Trends in Mechanical Engineering, Gujarat, India, 6–7 July 2017.
11. Weber, M.; Vorwerk, C. Neuartiges antriebskonzept zum fahren, lenken und heben. *Log. J. Proc.* **2010**, *6*. [CrossRef]
12. Melkus, A. Fahreloses transportfarzeug: EP, No. EP3216747A1. 7 March 2016.
13. F3-Design. Available online: https://www.dinostretchhood.com/nipper/ (accessed on 21 November 2018).
14. AGILOX SYSTEM. Available online: http://agilox.net/ (accessed on 19 July 2018).
15. Hassan, K.K. *Nonlinear Systems*, 3rd ed.; Prentice Hall: Englewood, IL, USA, 2002; pp. 551–625.

16. Kim, S.; Kwon, S. Nonlinear Control Design for a Two-Wheeled Balancing Robot. In Proceedings of the 2013 10th International Conference on Ubiquitous Robots and Ambient Intelligence, Jeju, Korea, 30 October–2 November 2013; pp. 486–487.
17. Osama, J.; Mohsin, J.; Yasar, A.; Khubab, A. Modeling, Control of a two-Wheeled Self-Balancing Robot. In Proceedings of the IEEE International Conference on Robotics and Emerging Allied Technologies in Engineering (iCREATE), Islamabad, Pakistan, 22–24 April 2014.
18. Antonio, H.J.; Yu, W. High-Gain Observer-Based PD COntrol for Robot Manipulator. In Proceedings of the IEEE Xplore Conference on American Control Conference, Chicago, IL, USA, 28–30 June 2000; Volume 4, pp. 2518–2522.
19. Voos, H. Nonlinear Control of a Quadrotor micro-UAV Using Feedback-Linearization. In Proceedings of the IEEE International Conference on Mechatronics, Malaga, Spain, 14–17 April 2009; pp. 1–6.
20. Goodarzi, F.; Lee, D.; Lee, T. Geometric Nonlinear PID Control of a Quadrotor UAV on SE(3). In Proceedings of the 2013 European Control Conference (ECC), Zürich, Switzerland, 17–19 July 2013; pp. 3845–3850.
21. Hu, Q.; Fei, Q.; Wu, Q. Research and application of nonlinear control techniques for quad rotor UAV. *J. Univ. Sci. Technol. China* **2012**, *42*, 706–710.
22. Young, K.D.; Utkin, V.I.; Ozguner, U. A control engineer's guide to sliding mode control. *IEEE Trans. Control Syst. Technol.* **1999**, *7*, 328–342. [CrossRef]
23. Boizot, N.; Busvelle, E.; Gauthier, J.P. An adaptive high-gain observer for nonlinear systems. *Automatica* **2010**, *46*, 1483–1488. [CrossRef]